Supplement Material for Robust AMD Stage Grading with Exclusively OCTA Modality Leveraging 3D Volume

Haochen Zhang[1], Anna Heinke[2], Carlo Miguel B. Galang[2], Daniel N. Deussen[2], Bo Wen[1], Dirk-Uwe G. Bartsch[2], William R. Freeman[2], Truong Q. Nguyen[1], Cheolhong An[1]
[1]Electrical and Computer Engineering Department, UC San Diego
[2]Jacobs Retina Center, Shiley Eye Institute, UC San Diego
{haz035, tqn001, chan}@ucsd.edu {aheinke, dbartsch, wrfreeman}@health.ucsd.edu

Table 1. Comparison of public **OCTA** datasets with the dataset collected by us.

OCTA dataset	Task	2D/3D	# of samples	# of AMD
PREVENT[3]	Segmentation	2D only	55	Unkown
ROSE [5]	Segmentation	2D only	229	Unkown
OCTAGON [3]	Segmentation	2D only	213	0
FOCTAIR [3]	Registration	2D only	86	Unkown
OCTA-500 [4]	Segmentation	3D and 2D	500	49
Ours	Classification	3D and 2D	889	749

1. Statistic of available OCTA dataset

Table 1 gives a comparison of public OCTA datasets with the dataset collected by us. Since most public datasets are designed for segmentation tasks and contain only a few samples of AMD, they are not applicable to perform OCTA-based AMD classification. In contrast, our dataset is specifically curated for AMD stage grading and has the largest number of total and AMD samples available. We observed the existence of a large-scale OCTA dataset, COIPS [6], but it is currently not publicly available.

In detail, our dataset comprises a total of 310 patients, spanning an age range from 30 to 101 years, with an average age of 76.6 years. Due to the inclusion of multiple scans from certain patients taken at different time points, we obtain a total of 893 scans. After a rigorous quality assessment that led to the removal of samples of subpar quality, we arrived at a refined set of 889 samples in our dataset utilized in all experimental analyses. This dataset has distribution as follows: Active-321, Remission-187, Dry-241, and Normal-140.

2. Experimental dataset details

Fig. 1 shows the data amount of datasets used in our experiments. 'w/' and 'w/o' denote samples with and without layer segmentation errors respectively. 'Unknown' refers to samples with no available error annotations. On the left, to keep the data amount same, we created the 'Mixed' sub-dataset by replacing error-free samples in the 'Clean' sub-dataset with samples containing errors. On the right, the error-free test set only contains samples without errors, while the error-prone test set includes samples with errors in all AMD stages. For the error-free training set, we removed all known samples with errors to build a relatively error-free set while maintaining the size of training set. For the error-prone training set, all samples except those used for testing were included.

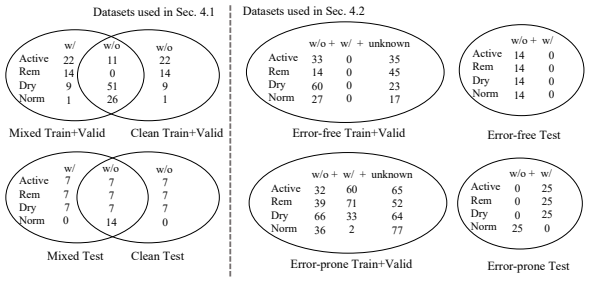

Figure 1. Illustration of the datasets used in our experiments

3. Human expert evaluation

Evaluation of OCTA images was performed by two masked retina specialists who regularly employ OCTA in clinical settings. These specialists assessed the presence or absence of CNV on OCTA en-face projections only and remained blind to other images (SD-OCT B-scan, OCT en-face scan), as well as clinical information. It's crucial to note that these graders were different from the retina specialists engaged in data labeling.

To predict the clinical category (Active, Remission, Dry AMD, and Normal), the masked graders focused exclusively on OCTA en-face projections, including the super-

[3]https://datashare.ed.ac.uk/handle/10283/3528

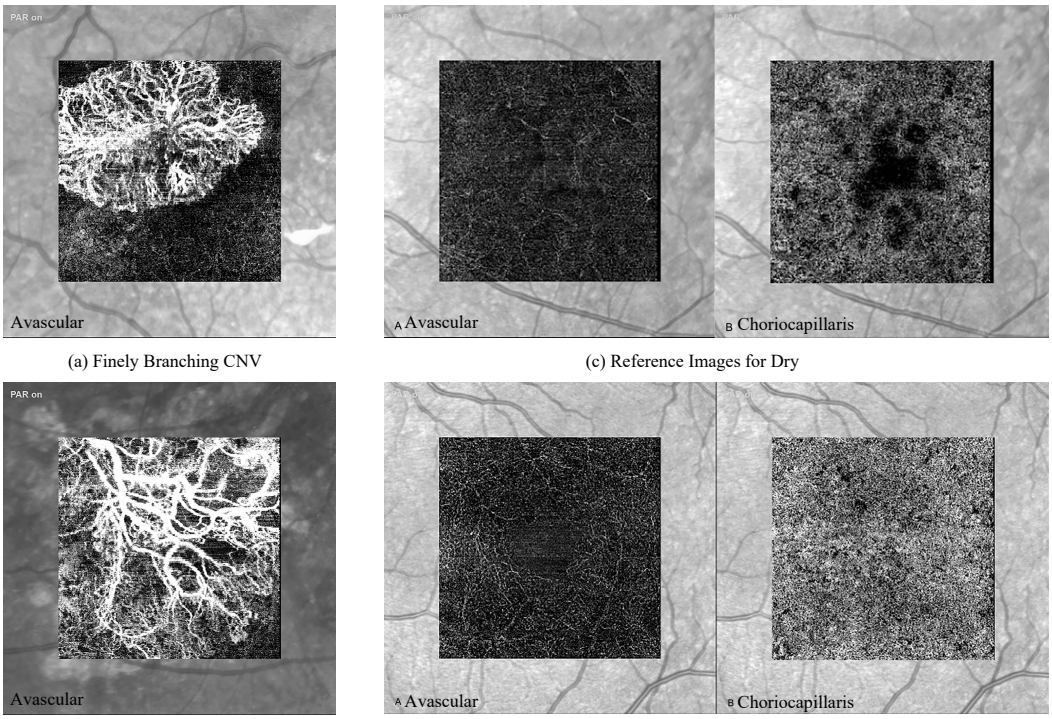

(a) Finely Branching CNV

(c) Reference Images for Dry

(b) Less Branching and More Mature

(d) Reference Images for Healthy Individual

Figure 2. Standardized reference images used in human expert evaluation experiment.

ficial vascular complex, deep vascular complex, avascular layer, and choriocapillaris. Initially, the presence or absence of CNV was determined using standardized reference images, comprising en-face structural OCTA images of the superficial inner retinal plexus, deep inner retinal plexus, outer retina, and choriocapillaris for each eye. Images indicating an evident neovascular plexus in the avascular layer and/or choriocapillaris were interpreted as indicating CNV presence. Subsequently, if vessels were detected, graders scrutinized their morphology, attempting to classify them as finely branching (presumably active, as depicted in Fig. 2a) or less branching and more mature (predominantly inactive, as illustrated in Fig. 2b). This classification was based on characteristics previously described by Coscas et al [2]. for reference, aiding in distinguishing the clinical category. Additionally, reference images for other categories were employed, such as Fig. 2c, showcasing OCTA in a patient with dry AMD, as characterized by Arya et al.[1]. Fig. 2d demonstrated a healthy individual with normal choriocapillaris and avascular layer in the OCTA en-face projection. These references, coupled with their clinical acumen, enabled the two expert graders to arrive at a consensus grading for predicting the four categories. Remarkably, the same 56 samples that the network classifiers used for testing were utilized by these two masked human graders to predict the category.

References

[1] Malvika Arya, Almyr S Sabrosa, Jay S Duker, and Nadia K Waheed. Choriocapillaris changes in dry age-related macular degeneration and geographic atrophy: A review. *Eye and Vision*, 5(1):1–7, 2018.

[2] Gabriel J Coscas, Marco Lupidi, Florence Coscas, Carlo Cagini, and Eric H Souied. Optical coherence tomography angiography versus traditional multimodal imaging in assessing the activity of exudative age-related macular degeneration: a new diagnostic challenge. *Retina*, 35(11):2219–2228, 2015.

[3] Macarena Díaz, Jorge Novo, Manuel G Penedo, and Marcos Ortega. Automatic extraction of vascularity measurements using OCT-A images. *Procedia Computer Science*, 126:273–281, 2018.

[4] Mingchao Li, Yuhan Zhang, Zexuan Ji, Keren Xie, Songtao Yuan, Qinghuai Liu, and Qiang Chen. IPN-v2 and OCTA-500: Methodology and dataset for retinal image segmentation. *arXiv preprint arXiv:2012.07261*, 2020.

[5] Yuhui Ma, Huaying Hao, Jianyang Xie, Huazhu Fu, Jiong Zhang, Jianlong Yang, Zhen Wang, Jiang Liu, Yalin Zheng, and Yitian Zhao. ROSE: A retinal oct-angiography vessel segmentation dataset and new model. *IEEE transactions on medical imaging*, 40(3):928–939, 2020.

[6] Yufei Wang, Yiqing Shen, Meng Yuan, Jing Xu, Bin Yang, Chi Liu, Wenjia Cai, Weijing Cheng, and Wei Wang. A deep learning-based quality assessment and segmentation system with a large-scale benchmark dataset for optical coherence tomographic angiography image. *arXiv preprint arXiv:2107.10476*, 2021.